Temperature dependence of electron mobility in GaAs-$Ga_{1-x}Al_xAs$ modulation-doped quantum wells

C. Guillemot, M. Baudet, M. Gauneau, and A. Regreny
Centre National d'Etudes des Télécommunications, 22301 Lannion Cédex, France

J. C. Portal
Laboratoire de Physique des Solides, Institut National des Sciences Appliquées, Université Paul Sabatier, 31077 Toulouse, France, and Service National des Champs Intenses, Centre National de la Recherche Scientifique, 38041 Grenoble Cédex, France

(Received 14 July 1986; revised manuscript received 30 September 1986)

We report the temperature dependence of the drift mobility in GaAs-$Ga_{1-x}Al_xAs$ modulation-doped quantum wells. A theoretical model is formulated that includes scattering by residual impurities located in the well, in the barrier, and at the "inverted" interface, by Si donors and acoustic phonons. Contributions to the total mobility arising from the segregated Si profile and background impurities piled up at the inverted interface are separated by secondary-ion mass spectrometry experiments and measurements of the temperature dependence of the scattering rate. The density of scattering centers trapped at the inverted interface increases with alloy composition x, independently of the $Ga_{1-x}Al_xAs$ barrier thickness.

I. INTRODUCTION

The properties of two-dimensional electron gases have been widely studied owing to the development of epitaxial techniques; basic results in this field have been reviewed by Ando, Fowler, and Stern.[1] Because of its unique transport characteristics, the two-dimensional electron gas confined at a GaAs-$Ga_{1-x}Al_xAs$ interface has received a great deal of attention and has given rise to a new generation of high-speed semiconductor devices such as the two-dimensional-electron-gas field-effect transistor. Thus, in a modulation-doped GaAs-$Ga_{1-x}Al_xAs$ heterojunction, electrons confined at the GaAs side of the interface and separated from their parent donors located in the $Ga_{1-x}Al_xAs$ side have exhibited low-field mobilities as high as 2×10^6 cm^2/V s at 4.2 K.[2]

The enhanced mobilities in these structures, however, do not necessarily satisfy all device requirements. The mobilities have been found to decrease drastically with an increase of the electric field, limiting the maximum current that can flow in the channel. In this respect, a modulation-doped double-heterojunction quantum-well structure has various advantages such as an electronic density twice as large as that of the single heterojunction and a channel thickness which is well defined, eliminating the short-channel effect.[3] However, since the pioneering work of Dingle *et al.*,[4] modulation-doped quantum wells have stimulated far fewer experimental transport studies than have single heterojunctions.[5–8]

Actually, the molecular-beam-epitaxial (MBE) growth of high-quality modulation-doped multiquantum-well structures is not a trivial process, since the structures contain the so-called "inverted" heterojunction, GaAs on $Ga_{1-x}Al_xAs$. Very high electron mobilities are thought difficult to achieve in the presence of the "inverted" interface for two main reasons. Photoluminescence studies[9] suggest that an impurity (probably carbon) is pushed forward in the growth direction as the $Ga_{1-x}Al_xAs$-vacuum interface advances, accumulates on this interface and is then trapped in the first few unit cells of GaAs when the Al flux is turned off. On the other hand, there is evidence[8,10,11] of surface segregation of silicon occurring for samples grown at a high substrate temperature, which gives rise to a diffused profile of doped Si impurities.

Besides these points, the properties of a two-dimensional electron gas are greatly affected by its screening behavior. The wave-vector and temperature dependence of the screening dielectric function contributes to a temperature-dependent part of the scattering rates that increases with temperature.[12] This contribution is also impurity-position dependent:[13] screening of impurities decreases with temperature faster for impurities located far in the barrier than for impurities within the electron gas, and this effect is all the more pronounced when the electron concentration is low.

The aim of this paper is to investigate the drift mobility as a function of the spacer width and temperature, especially for a rather-low-electron-concentration sample. Thus, we expect to change the relative contributions to the mobility of silicon and impurities trapped at the "inverted interface." In the studied samples, the spacer width varies from 220 to 650 Å and the electron concentration is about 3.2×10^{11} cm^{-2} with the exception of one sample where it is 1.6×10^{11} cm^{-2} electrons. Mobilities have been measured between 4.2 and 77 K.

In Sec. II, the quantum background is described and we calculate the electron eigen-wave-functions and their eigenenergies. We give the relaxation times for impurities and acoustic phonons screened by the random-phase-approximation (RPA) dielectric function at finite temperature. In Sec. III, we discuss the characterization of the samples and we examine the different parameters af-

fecting the electron mobility. Experimental and theoretical results are compared in Sec. IV A summary and conclusions are given in the last section.

II. QUANTUM BACKGROUND AND MOBILITY

Because of the barrier thickness, interactions between adjacent wells are negligible and electron properties are studied in one GaAs well surrounded by doped $Ga_{1-x}Al_xAs$ layers. Thus, we consider a quantum well of width L and barrier height V_ω while n_e is the free-electron-gas density. In the following, a uniform background dielectric constant κ is assumed and the in-plane electronic properties are described with a GaAs effective mass m^*. In the Hartree approximation, the electronic Hamiltonian for the envelope function is given by

$$H=(p_x^2+p_y^2)/2m^*+H_{sq}+V_e(z)\ , \tag{1}$$

$$H_{sq}=p_z^2/2m+V_\omega H(|z|-L/2)\ . \tag{2}$$

The well center is taken as the z origin and H is the Heaviside step function. Assuming the continuity of the eigenstates Ψ^{sq} of (2) and of the corresponding probability current at the interfaces,[14] we obtain the well-known eigenvalues and eigenstates of the square-well Hamiltonian. The even bound states are

$$i=0,2,4,\ldots\ ,$$

$$\Psi_i^{sq}(z)=A\cos(k_iz),\quad |z|<L/2$$

$$\Psi_i^{sq}(z)=B\exp[-K_i(z-L/2)],\quad z>L/2$$

$$\Psi_i^{sq}(-z)=\Psi_i^{sq}(z)\ ,$$

and

$$E_i^{sq}=\hbar^2k_i^2/2m^*\ ,$$

$$E_i^{sq}=V_\omega-h^2K_i^2/2m_b\ ,$$

$$k_i\tan(k_iL/2)/m^*=(K_iL/2)/m_b\ ,$$

where m_b is the barrier effective mass. $V_e(z)$ is the Hartree potential due to the free-carrier charge. If we assume that the ground subband is the only populated one, this Hartree potential is related to the ground eigenfunction via the Poisson equation. We solved the eigenstate equation and the Poisson equation self-consistently in the restricted basis (Ψ_0^{sq}, Ψ_1^{sq}, Ψ_2^{sq}). V_e is even and couples Ψ_0^{sq} and Ψ_2^{sq}. If the second excited bound state Ψ_2^{sq} does not exist, we apply the first-order nondegenerated perturbation V_e on E_0^{sq}. Finally, the chemical potential μ at the temperature T is given by

$$\mu=k_BT\ln[\exp(\mu_{k_BT=0}/k_BT)-1]\ ,$$

with

$$\mu_{k_BT=0}=\pi\hbar^2n_e/m^*\ .$$

Electrons interact with different ionized impurities: residual impurities in the whole structure, donors located in the barrier, or interface impurities. Each of them gives rise to a screened Coulombic potential and, thus, to an energy-dependent scattering rate

$$1/\tau_i(\varepsilon)=(2\pi/\hbar)(e^2/4\pi\epsilon_0\kappa)^2(1/\varepsilon)\int_0^{2\sqrt{\varepsilon}}dqg^2(q,z_i)q^2/\{[q\epsilon_{RPA}(q)]^2(4\varepsilon-q^2)^{0.5}\}\ ,$$

where $g(q,z_i)$ is related to the screening Hartree potential undergone by an impurity located at z_i and is given by

$$g(q,z_i)=\int_{-\infty}^{\infty}\Psi_0^2(z)\exp(-q|z-z_i|)dz\ .$$

At low temperatures (<70 K), the lattice scatters electrons essentially by acoustic mode phonons through the deformation potential Γ and the piezoelectric field.[15] Although it has been shown[16] that the dominant electron—optic-phonon interaction involves phonon modes associated with the interfaces, acoustic phonons are supposed to be those of bulk GaAs and isotropic. Since at very low temperatures, the mobility is dominated by impurity scattering, phonon-scattering rates are calculated out of the Bloch range. This being granted, we have

$$1/\tau_{def}(\varepsilon)=(3/4\pi\hbar)(\Gamma^2k_BT/\rho v_s^2L_{eff})(1/\varepsilon)\int_0^{2\sqrt{\varepsilon}}dqq^4/\{[q\epsilon_{RPA}(q)]^2(4\varepsilon-q^2)^{0.5}\}\ ,$$

where ρ is the mass density, v_s the longitudinal velocity of sound, and L_{eff} an effective well width given by

$$L_{eff}=3\pi\Big/\left[\int_{-\infty}^{\infty}dq\left[\int dz\Psi_0^2(z)\exp(iqz)\right]^2\right]\ ,$$

$$1/\tau_{piezo}(\varepsilon)=(1/4\pi\hbar)(eh_{14})^2(k_BT/\rho v_s^2)[\tfrac{9}{32}+(v_s/v_t)^2\tfrac{13}{32}](1/\varepsilon)\int_0^{2\sqrt{\varepsilon}}dqq^3/\{[q\epsilon_{RPA}(q)]^2(4\varepsilon-q^2)^{0.5}\}\ ,$$

where h_{14} is the basic piezoelectric tensor component and v_t is the transverse velocity of sound. Alloy disorder scattering arises from the wave-function extension into the $Ga_{1-x}Al_xAs$ layer,[17]

$$1/\tau_{al}(\varepsilon)=(1/2\pi\hbar)x(1-x)(a^4/4)\Delta E_c^2 2\int_0^{\infty}dz\Psi_0^4(z)(1/\varepsilon)\int_0^{2\sqrt{\varepsilon}}dqq^4/\{[q\epsilon_{RPA}(q)]^2(4\varepsilon-q^2)^{0.5}\}\ ,$$

where x is the percentage of aluminum, ΔE_c the difference of the band conduction minima, a the lattice constant. In the preceding equations, $\epsilon_{RPA}(q)$ is the RPA dielectric function:

$$\epsilon_{RPA}(q)=1+(e^2/\epsilon_0\kappa q)f(q)\Pi_{RPA}(q)\ .$$

Π_{RPA} is the RPA polarizability and is calculated at finite temperature using Maldague's method.[18] $f(q)$ is a form

factor taking into account the finite extension of the function $\Psi_0(z)$:

$$f(q)=\int\int dz\,dz'\Psi_0^2(z)\Psi_0^2(z')\exp(-q\,|\,z-z'\,|\,)\ .$$

Finally, the scattering time is calculated by integrating the total energy-dependent scattering time over the Fermi distribution.

Dominant scattering mechanisms limiting the mobility of a two-dimensional electron gas have been the subject of many recent studies. The temperature dependence of the electron mobility has been used to characterize the interplay between screened impurity scattering and acoustic phonon scattering in a single modulation-doped heterojunction.[19–21] To select between surface roughness and remote impurity scattering, Harrang *et al.* calculated the ratio of the quantum-to-classical scattering time.[22] The classical scattering time is derived from the drift mobility and is given by

$$1/\tau_c=\int dk' W_{k,k'}(1-\cos\theta)\ ,$$

where $W_{k,k'}$ is the probability of scattering from state k to state k' and θ is the scattering angle. The classical time favors large-angle scattering over small-angle scattering due to the weighting factor of $1-\cos\theta$. The quantum scattering time is deduced from the Shubnikov–de Haas oscillation envelope and is expressed as

$$1/\tau_q=\int dk' W_{k,k'}\ .$$

Since we are interested in selecting the dominant impurity scattering rate involved in the total mobility, a crude calculation has been performed in order to estimate the sensitivity of the quantum-to-classical scattering-time ratio to the impurity position. The unscreened form of the differential cross section is used and the eigen-wavefunction extension in the growth direction is ignored. Then,

$$\tau_q/\tau_c=\int_0^{2\pi} d\theta\sigma(\theta)[1-\cos(\theta)]\exp[-2\sin(\theta/2)kz_i]/2\int_{\theta_c}^{\pi} d\theta\sigma(\theta)\exp[-2\sin(\theta/2)kz_i]$$

where z_i is the impurity position and $\sigma(\theta)$ is the differential cross section in two dimensions:[23]

$$\sigma(\theta)=G\tanh(\pi G)/2k\sin^2(\theta/2)\ ,$$

where

$$G=m^*e^2/k\kappa\hbar^2\ .$$

For a two-dimensional-electron-gas density of 3×10^{11} cm^{-2}, the critical angle θ_c is about 10° (Ref. 22) and k at the Fermi level is 1.37×10^6 cm^{-1}. The expected ratio of τ_q/τ_c is 0.13 for an interface impurity ($z_i=100$ Å) and 0.11 for a remote impurity ($z_i=400$ Å). The difference between the calculated scattering-time ratios is rather small and would not allow to measure the interplay between remote-Si-donor scattering and interface-impurity scattering. In both cases small-angle scattering is favored over large-angle scattering.

On the other hand, we have investigated the temperature dependence of the electron mobility. Because of the wave vector dependence of the screening dielectric function, any impurity scattering rate increases as the temperature is raised.[12] However, the increase rate is impurity-position dependent. Figure 1 shows the differences occurring for an impurity located at the center of the well, at the interface or far in the barrier. The parameters used in the calculations are those of the low electron density sample and the energy ϵ is the Fermi level at $T=0$ K. The scattering rate increase is all the more pronounced as the impurity is out of the electron gas. Since the RPA is a linear approximation, the screening potential is weaker for a potential weakly interacting with the electron gas than for an impurity located inside or near the well. Thus, the temperature influence on the strong screening potential associated with an impurity located in the well is weak. What is more, the temperature dependence of screening increases as electron density decreases since screening is no more saturated at the Thomas-Fermi limit.[13] Then the impurity position dependence is all the more well-marked as the electron concentration is low (Fig. 2). This behavior is qualitatively independent of the electron energy ϵ. However, its amplitude increases with ϵ and then with temperature, since the electron mean energy increases as the temperature is raised. Bearing in

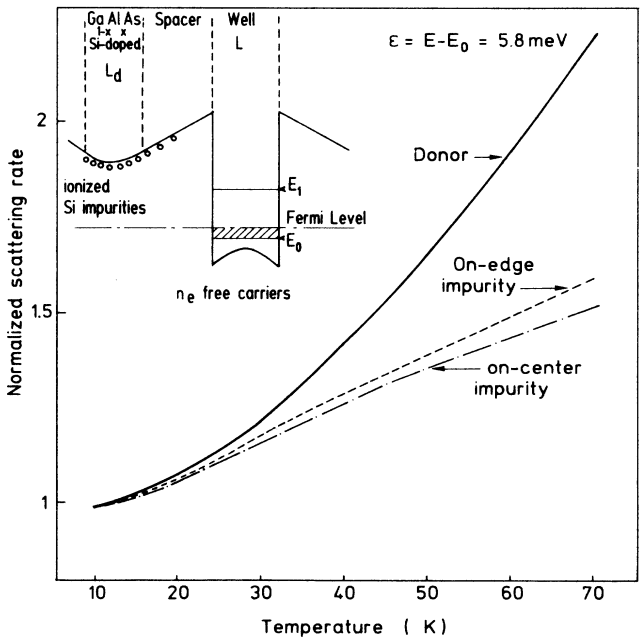

FIG. 1. Dependence of the normalized scattering rate $[1/\tau_i(T)]/[1/\tau_i(10\ \mathrm{K})]$ for an impurity located at the well center ($z_i=0$), at the edge ($z_i=L/2$) and in the barrier ($z_i=L/2+L_b/2$). Scattering rates are calculated for an energy $\varepsilon=5.8$ meV. The parameters used are (sample No. 6): $L=161$ Å, $L_b=783$ Å, $n_e=1.63\times10^{11}$ cm^{-2}, $E_0=19$ meV.

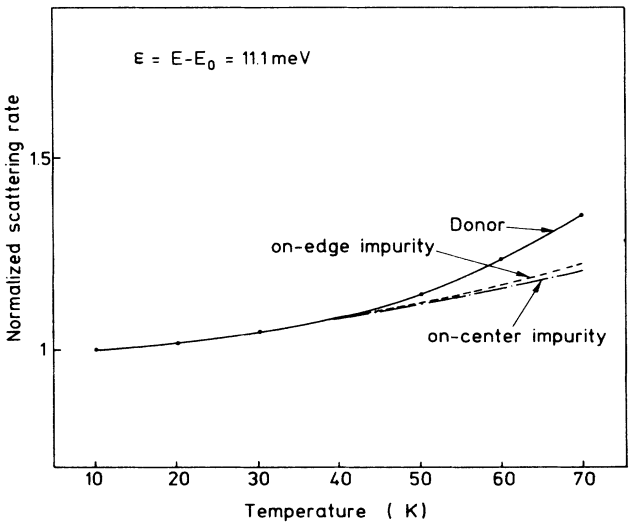

FIG. 2. Dependence of the normalized scattering rate $[1/\tau_i(T)]/[1/\tau_i(10\ \mathrm{K})]$ for an impurity located at the well center ($z_i=0$), at the edge ($z_i=L/2$) and in the barrier ($z_i=L/2+L_b/2$). Scattering rates are calculated for an energy $\varepsilon=11.1$ meV. The parameters used are (sample No. 5): $L=158$ Å, $L_b=856$ Å, $n_e=3.11\times10^{11}$ cm^{-2}, $E_0=23.1$ meV.

mind the above considerations, the experimental mobility will be now analyzed.

III. SAMPLES CHARACTERIZATION

The samples were grown in a home-modified MBE Riber reactor equipped with a multiple sample interlock, on Cr-doped semi-insulating GaAs(100) at a substrate temperature of 690 °C. A 1-μm GaAs buffer layer is followed by 1000 Å of undoped $Ga_{1-x}Al_xAs$ to avoid electron accumulation at this heterointerface. Then comes an 11-period selectively doped multiple-quantum-well (MQW) structure made of a Si-doped $Ga_{1-x}Al_xAs$ layer and a GaAs well surrounded by undoped $Ga_{1-x}Al_xAs$ spacers (see the inset in Fig. 1). Finally there is a surface layer of 300 Å of doped $Ga_{1-x}Al_xAs$ and 220 Å of doped GaAs where should be confined the surface band bending due to surface defects. The same doping level N_d was used in the whole structure.

X-ray diffraction methods allow us to directly obtain the average Al composition $x_a=xL_b/(L+L_b)$, where L_b is the barrier thickness, and the period $L+L_b$. The values of x, L, and L_b are then determined by fitting calculated and experimental intensities of x-ray peaks.[24] From L_b, we infer the spacer and the doped-$Ga_{1-x}Al_xAs$ thicknesses. Results are reported in Table I.

Mobility and sheet electron concentration were measured first on the whole sample, by the Van der Pauw method at 4.2 K. Then samples were photolithographically made into Hall bridges 300 μm long. Comparing Van der Pauw and Hall results allows us to infer sample homogeneity. Magnetic field strength never exceeded 500 G and voltages were kept below 10 mV. Ohmic contacts were made by alloying In at 450 °C in an H_2 atmosphere. Measurements were performed in the dark and under illumination at 4.2 K. A weak persistent photoconductivity effect was recorded.

In addition, Shubnikov–de Haas measurements were performed on all samples. Apart from spin splitting at high magnetic fields, no evidence of oscillations other than those of the main period was found. This shows that only a single sheet of electrons per well contributes[8] to the mobility and that the electron concentration is similar in all the wells. This allows us to calculate electron density per well from 4.2-K Hall data and to compare it to Shubnikov–de Haas results. A good agreement appears from the results in Table I that show that at least 10 wells are connected by In contacts.

Assuming a complete depletion of the barriers, we get from the doped $Ga_{1-x}Al_xAs$ thickness L_d and the electron density, the doping level for each sample: $N_d=n_e/L_d$. From this value and with ΔE_c being 60% of the band gap,[25] it is easily established that the Fermi level is below the Si donor level in the barrier, confirming our previous hypothesis, excepted for sample No. 4. In this case, the barrier is partially depleted. Moreover, the doping levels of Table I are consistent within 5%, with a reference doped $Ga_{1-x}Al_xAs$ bulk sample measured by the Van der Pauw method and secondary ion mass spectroscopy (SIMS). They both give $N_d=2.6\times10^{17}$ cm^{-3}. SIMS measurements were performed to determine the Si depth profiles. The determination were carried out with a cesium primary beam which gives a good sensitivity for Si, above 10^{15} cm^{-3}, and avoids the deleterious effect of the AlH^- interfering ions. The data were calibrated by integrating the areas of Si profiles registered in nonannealed Si-implanted standards. The precision on the im-

TABLE I. This table gives the structural parameters of the samples deduced from x-ray measurements, the calculated lower eigen energies, the calculated doping level, the measured electronic densities and the segregation length deduced from Si SIMS profiles. The precisions of x-ray derived parameters is about 10%.

Sample No.	Well thickness L (Å)	Barrier thickness L_b (Å)	Doped $Ga_{1-x}Al_xAs$ L_d (Å)	Spacer (Å)	x	E_0 (meV)	E_1 (meV)	N_d (10^{17} cm^{-3})	n_e (Hall) (10^{11} cm^{-2})	n_e (Shubnikov) (10^{11} cm^{-2})	Mobility (4.2 K) (m^2/V s)	L_s (Å)
1	220	548	110	219	0.28	21	44.8	2.76	3.01	3.18	6.4	105
2	252	875	125	375	0.25	22.3	40.1	2.76	3.25	3.65	19.4	110
3	274	1089	121	484	0.24	21.9	37	2.75	3.15	3.51	29	100
4	274	1412	128	642	0.21	19	34		2.5	2.74	9.24	
5	158	856	122	367	0.21	23.1	63.1	2.56	3.09	3.13	19.7	
6	161	784	60	362	0.223	19	59.5	2.72	1.64	1.62	12.6	

purity concentration is estimated to be about 20% and to be reached after 20 Å of doped material.

To characterize bulk materials, several unintentionally doped GaAs samples have been measured by the Van der Pauw method. The samples were always p-type with p ranging from 1×10^{14} to 4×10^{14} cm^{-3} and mobility varies between 380 and 400 cm^2/V s at 300 K. Then, to analyze experimental quantum wells mobilities, we estimate the GaAs total residual impurity level to be 5×10^{14} cm^{-3}. An unintentionally doped $Ga_{1-x}Al_xAs$ layer with $x=0.28$ was grown. This sample is also p type with 1.25×10^{14} cm^{-3} holes and a 300-K mobility of 300 cm^2/V s. The $Ga_{1-x}Al_xAs$ total residual impurity level has been evaluated to be 10^{15} cm^{-3}. We will come back to these points later.

The last impurity contribution to mobility comes from potential interface scattering centers. Photoluminescence of unintentionally doped quantum wells,[9] reveals the incorporation of acceptors (C or O) near the interfaces while transmission electron microscopy performed on quantum well superlattices relates interface roughness to trapped impurities at the quantum well interfaces.[26] They should originate either from the substrate or from the $Ga_{1-x}Al_xAs$ MBE layers. We will suppose in the following, that they are incorporated in the first 20 Å of GaAs following $Ga_{1-x}Al_xAs$ layers. This value seems reasonable and is not crucial.

The deformation potential Γ has been reported to range between 7 and 16 eV in GaAs. A deformation potential of 13.5 eV in modulation-doped single heterojunctions has been shown consistent with a theoretical model for the acoustic-phonon limited mobility that includes screening.[19,20] From the analysis of the energy relaxation of two-dimensional hot electrons, it has been recently derived a deformation potential constant of 11 eV.[27] On the other hand, the electron mobility in two-dimensional electron gas has been successfully accounted for assuming a deformation potential of 7 eV and ignoring screening of the acoustic-phonon scattering potentials.[28,29] In our approach, Γ is a fitting parameter determined by mobility analysis in the same way as the interface impurity level. Other numerical material values are collected in Table II.[15]

IV. MOBILITY ANALYSIS

We now use the preceding results to compare the calculated and experimental values of the drift mobility. To determine, first of all, the deformation potential value, we fit the sample 3 experimental mobility to the theoretical one. Indeed, its high mobility implies that phonon diffusion quickly becomes the prevailing mechanism involved in the total scattering time. The interface impurity density is determined at the same time with the 4.2-K mobility value. Should Si donors segregate, it would not matter since all impurities give rise to similar temperature profiles for this 3.5×10^{11} cm^2 electron density sample. Moreover, this hypothesis will be tested back. We get a deformation potential Γ of 12.8 eV which is very close to the value of 13.5 eV obtained for single heterojunctions[19,20,27] and slightly lower than the GaAs value of 16 eV deduced from transport experiments.[30] Fitting, now, the mobility of the low-electron-density sample No. 6, without introducing Si segregation, we get a theoretical mobility which slightly increases with temperature from its 4.2-K value whereas the experimental mobility slightly decreases (see Fig. 3). So, we are led to raise the donor contribution to the mobility, since this contribution increases with temperature more slowly than others due to screening effects. The total donor scattering rate is increased by introducing Si dopant segregation in the growth direction. So, the effective spacer width is reduced for one side of the quantum well, near the "inverted" interface, whereas it is enlarged on the other side. In consequence, scattering on ionized silicon occurs mainly from dopants located at the "inverted" interface side. However, if the dopant segregation is overestimated, Si will be located mainly near the GaAs quantum well. Then, the related scattering rate will increase too slowly with temperature and the theoretical model will fail again in accounting for the experimental data.

Barnett *et al.* have elaborated a general model describing the incorporation of dopants into crystal films, grown by MBE which accounts for dopant surface segregation during deposition.[31] The model needs as input data, ther-

TABLE II. GaAs material parameters (see Ref. 15).

m^*/m_0	0.067
κ	12.90
ρv_l^2	1.40×10^{12} erg/cm^3
ρv_t^2	0.48×10^{12} erg/cm^3
h_{14}	1.2×10^7 V/cm

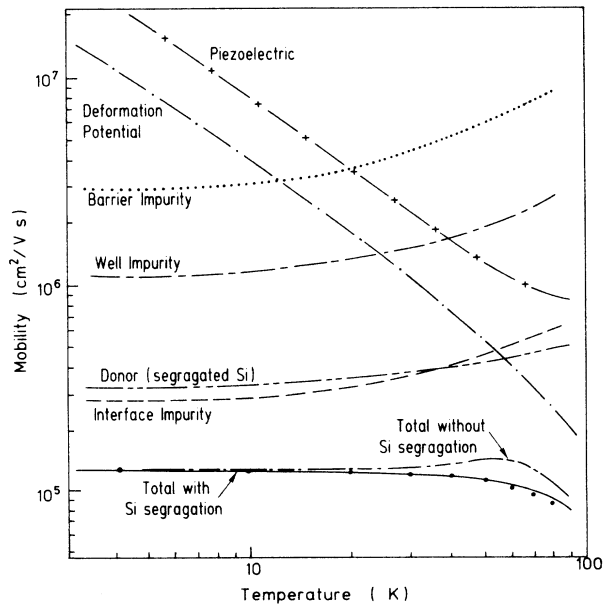

FIG. 3. Temperature dependence of the electron mobility for the low electron density sample (No. 6). Solid circles correspond to experimental data measured in the dark. Theoretical total mobilities with and without Si segregation are reported. The interface impurity density is 0.65×10^{10} cm^{-2}.

modynamic and kinetic parameters. Following the general idea of this model, we make the hypothesis that the Si incorporation probability is proportional to the Si surface density during the growth. Then we have

$$\tau(r)=L_s D(r) ,$$

$$d\tau=Fdt-Ddr ,$$

$$dr=v\,dt ,$$

which gives

$$D(r)=N_d[1-\exp(-r/L_s)],\quad 0<r<L_d$$

$$D(r)=D_{\max}\exp(-r/L_s),\quad r>L_d$$

$$D_{\max}=N_d[1-\exp(-L_d/L_s)] .$$

τ is the Si surface density, $D(z)$ the doping level, F the net Si impinging flux, and v the $Ga_{1-x}Al_xAs$ growth speed. We have

$$\int_0^\infty dr D(r)=N_d L_d ,$$

since segregation acts as an incorporation lag. This model can be used to analyze the dopant depth distribution profile and gives the maximum doping level $D_{\max}$ as a function of the unique unknown parameter L_s. Consequently, we have analyzed by SIMS experiments, three superlattice Si profiles (Fig. 4) and inferred L_s from $D_{\max}$ (Table I). The deduced value of 105 Å ranges between the respective values 60 and 175 Å of Ref. 8 and 32, for a growth substrate temperature of 690°C. Assuming the same behavior of Si in GaAs, the analysis of binding energies of Si donors confined in GaAs-$Ga_{1-x}Al_xAs$ quantum wells, leads to a segregation length of 50 Å.[33] The density of Si impurities incorporated in the GaAs well reaches 2.5×10^{10} cm^{-2} for sample No. 1 and the question arises whether or not these donors are ionized. For high-carrier concentrations ($>10^{11}$ cm^{-2}), the impurity binding energy is reduced to a very small value (<1 meV) by screening effects.[13] The overlap between electron bound states broadens the impurity band which merges into the conduction band.[34] Therefore the random-phase approximation (RPA) linear screening theory should be a correct approximation even for impurities located near and in the GaAs quantum well. Then, whether Si acts as a donor or an acceptor, it behaves as an ionized impurity scattering center.

A very good agreement between theory and experiment, occurs from the preceding conclusions for sample No. 6 (Fig. 3). The mobility profile of, sample No. 3 used in the deformation potential determination, is also displayed (Fig. 5). The unique fitting parameter is, now, the impurity interface density N_i which has been determined for each sample. A typical temperature dependence of the total electron mobility, resulting from the contributions of all scattering mechanisms, is shown on Fig. 6. It is seen that the interface impurity scattering is the dominant mechanism for T lower than 60 K before phonons prevail. No correlation comes out between N_i and the $Ga_{1-x}Al_xAs$ thickness but N_i increases almost linearly with the alloy composition x (Fig. 7). Finally, changing the residual impurity level or the Si segregation length in the GaAs up to 75 Å, does not strongly modify our conclusions. As an example, increasing the $Ga_{1-x}Al_xAs$

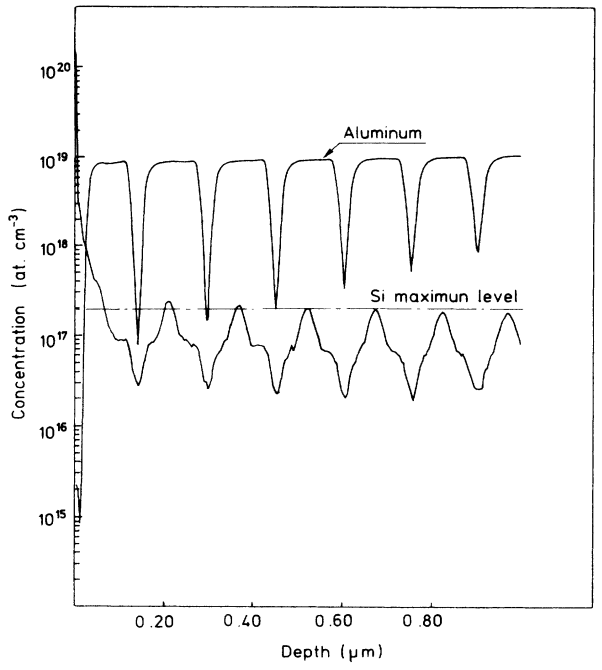

FIG. 4. Si and Al depth profiles analyzed by SIMS for sample No. 3. The recorded ions are polyatomic ions $^{54}Al_2^-$ and $^{28}Si^-$. The maximum level reached by Si concentration is reported.

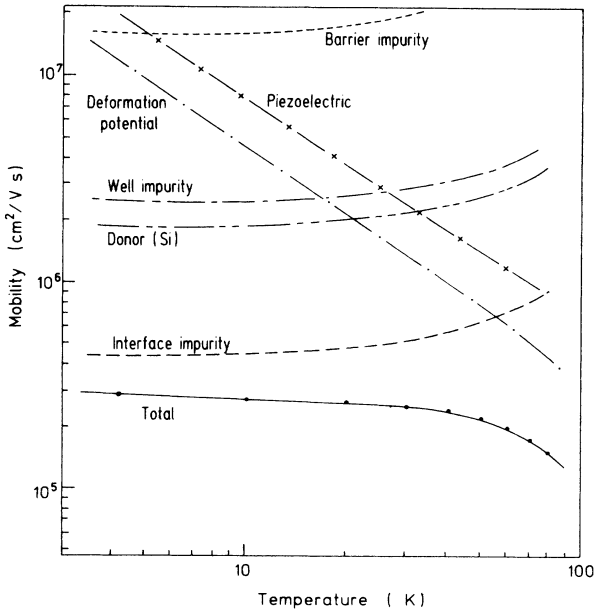

FIG. 5. Temperature dependence of the electron mobility for sample No. 3. Solid circles correspond to experimental data measured in the dark. Theoretical mobilities are reported. The interface impurity density is 2.25×10^{10} cm^{-2}.

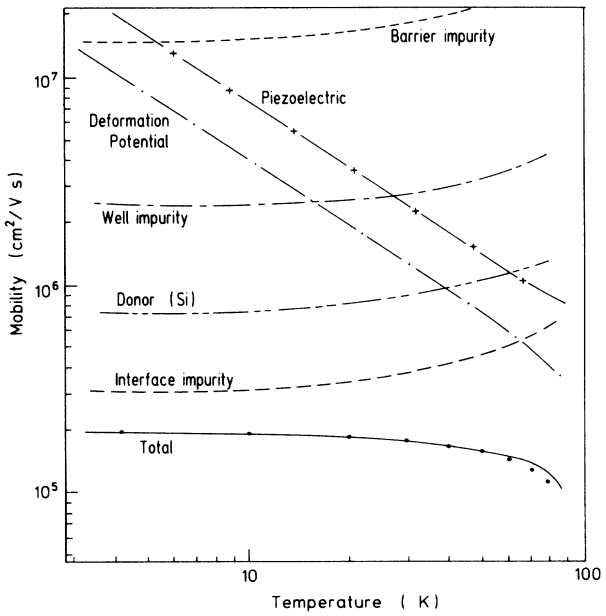

FIG. 6. Temperature dependence of the electron mobility for sample No. 2. Solid circles correspond to experimental data measured in the dark. Theoretical mobilities are reported. The interface impurity density is 3.25×10^{10} cm^{-2}.

background impurities level up to 5×10^{15} cm^{-3} decreases the interface density of sample 2 from 3.3 to 3×10^{10} cm^{-2}.

The diffused profile of doped-Si impurities and the charged centers located at the inverted interface, break the structure symmetry and couple Ψ_0 and Ψ_1^{sq}. However, because of the large width of the spacers and of the small values of N_i as compared to n_e, the electronic ground function should be weakly modified.

In order to determine whether interface impurities are located at both interfaces or not, we have calculated the mobility limited by interface ionized impurities in a single modulation doped heterojunction. We assume that electrons populate only the lowest subband and we adopt for the eigen-wave function $f(z)$ the Fang-Howard variational wave function,[23]

$$f(z)=(b^3z^2/2)^{1/2}\exp(-bz/2)\ .$$

The variational parameter b is given by

$$b=(12m^*e^2/\kappa\epsilon_0\hbar^2)^{1/3}(N_{\rm depl}+\tfrac{11}{32}n_e)^{1/3}\ ,$$

where $N_{\rm depl}$ is the areal concentration of depletion charges in the GAs. If we assume that the interface impurities are located at both interfaces in a quantum well, the area density of interface scattering centers is about 3.75×10^{10} cm^{-2} in a single heterojunction where the aluminum concentration of the barrier is 0.3. In Fig. 8, the zero-temperature mobility limited only by these interface ionized impurities, is plotted as a function of the electron density n_e. Previously reported measurements are also included. The theoretical curve lies about one order of magnitude below the experimental data recorded from "normal" heterojunctions except for two values. In conse-

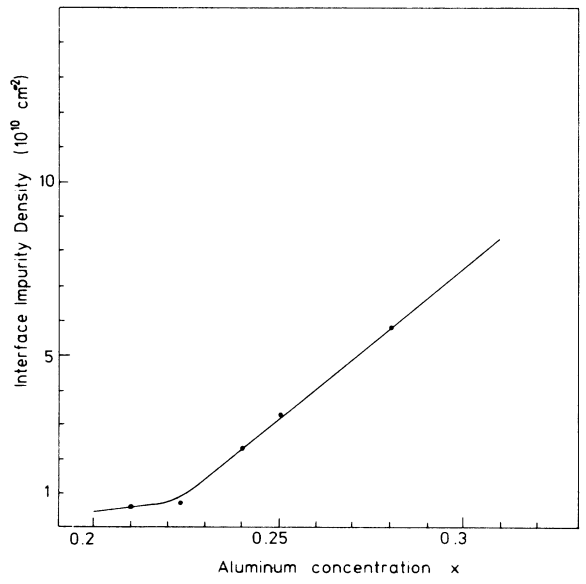

FIG. 7. Dependence of the interface impurity density with the barrier aluminum concentration. Solid circles correspond to values deduced from the mobility analysis.

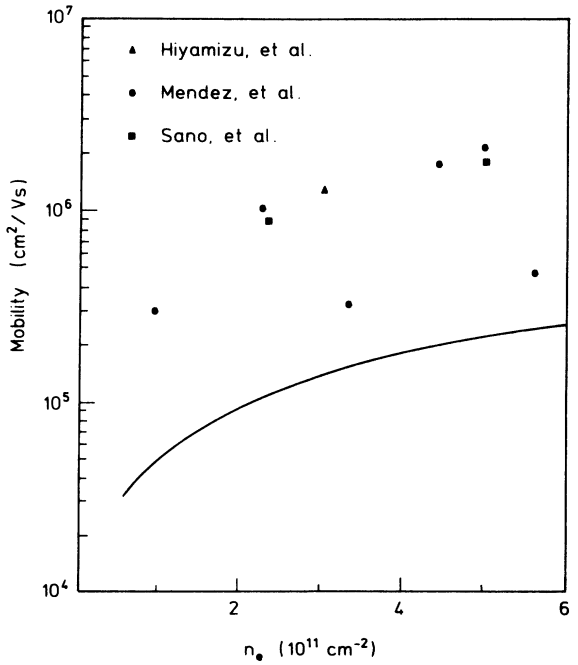

FIG. 8. Zero-temperature mobility as a function of the electron density in a single modulation-doped heterojunction. The area concentration of depletion charges in the GaAs is 6×10^{10} cm^{-2} and the aluminum concentration in the barrier is 0.3. The mobility is limited by 3.75×10^{10} cm^{-2} interface scattering centers. Also included are previously reported experimental data: Hiyamizu *et al.* (Ref. 2), Mendez *et al.* (Ref. 19), and Sano *et al.* (Ref. 35).

quence the incorporation of impurities at the "normal" interface $Ga_{1-x}Al_xAs$ on GaAs is ruled out. So, interface impurities densities reported on Fig. 7 are concerned only with the "inverted" interface.

Sample No. 4 has not been included in the precedings results; its mobility clearly does not fit the theoretical study: a weak aluminum concentration and a large spacer should not lead to a poor mobility. An additional scattering mechanism must obviously be introduced. Every sample has been found to be homogeneous except sample No. 3. In this case, its 4.2-K mobility ranges between 200 000 and 300 000 $cm^2/V\,s$. In order to test whether the poor mobility of sample No. 4 and the lack of homogeneity observed on sample No. 3 are related to the surface roughness of quantum wells, we have calculated the scattering effects of the discontinuities present at the interfaces. Assuming that the surface deviates from a plane by a distance $\delta z(r)$ in the z direction at the point r in the plane and assuming that these deviations have an autocorrelation function with rms height Δ and autocorrelation length Λ, then the scattering rate experienced by electrons is given by[17]

$$\hbar/\tau(\varepsilon)=(\Delta\Lambda F)^2(1/\varepsilon)\int_0^{2\sqrt{\varepsilon}} dq\, q^4 \exp(-q^2\Lambda^2/4)/\{[q\epsilon_{\mathrm{RPA}}(q)]^2(4\varepsilon-q^2)^{0.5}\}\ .$$

Here the deviations are not correlated from one interface to the other and the interfaces are supposed to behave similarly since the aluminum concentration is lower than 0.3.[36] F is an effective field including the modification due to the change of effective mass at each interface:[37]

$$F=V_\omega\Psi_0^2(L/2)+\hbar^2/2m^*[d\Psi_0^2/dz(L/2)](1-m_b/m^*)\ .$$

Interface growth steps have been shown to be of the order of one atomic monolayer high in samples grown in similar conditions.[38] Assuming a rms height Δ of 2.86 Å, the mobility limited by interface roughness has been calculated for three autocorrelation lengths (Fig. 9). Mobilities quickly increase with the well width and show minima values for an autocorrelation length $\Lambda=100$ Å. However theoretical mobilities are quite high and this model of interface roughness scattering is unable to explain the discrepancies of our experimental data. Moreover the treatment used here implicitly assumes that the deviations from a flat interface are small and smoothly varying.[35] High steps could occur at the "inverted" interface because of the large thickness of the $Ga_{1-x}Al_xAs$ barrier ($L_b > 1000$ Å) of samples No. 3 and No. 4. It seems that this theoretical treatment cannot account for large deviations from a flat interface.

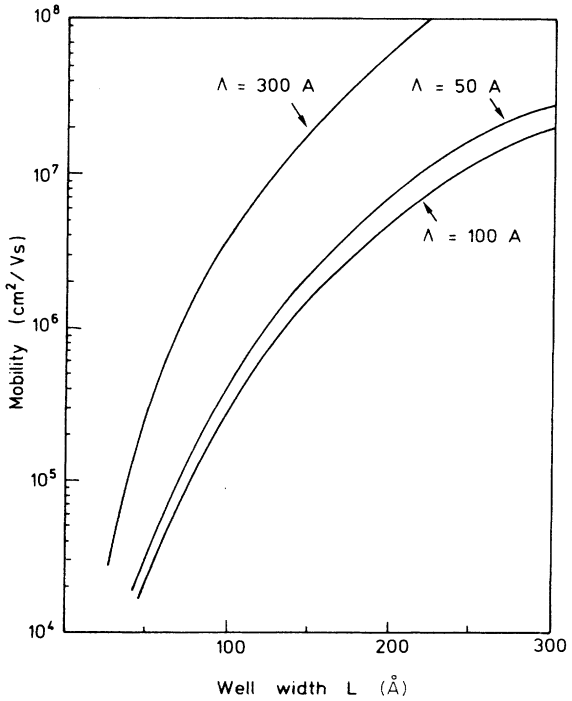

FIG. 9. Calculated mobility limited by interface roughness in a modulation-doped quantum well as a function of the well width. The standard deviation height is one atomic layer ($\Delta=2.86$ Å) and the results are reported for three auto correlation length Λ. The electron density is 3×10^{11} cm^{-2} and the barrier height is 200 meV.

V. CONCLUSION

We have performed an analysis of the different scattering mechanisms affecting the modulation-doped quantum-well mobility. Scattering occurs mainly from silicon segregation over about 105 Å and background impurities piled up at the inverted interface. It seems likely that carbon is trapped at the $Ga_{1-x}Al_xAs$-vacuum interface and would float on the $Ga_{1-x}Al_xAs$ film during growth giving rise to an interface impurity layer independent of the $Ga_{1-x}Al_xAs$ thickness. These impurities could inhibit $Ga_{1-x}Al_xAs$ growth by preventing lateral propagation of the atomic layer, leading to important interface roughness for large $Ga_{1-x}Al_xAs$ layer. In our samples, the $Ga_{1-x}Al_xAs$ layer is at least 550 Å thick and it would be of interest to check these conclusions for thin $Ga_{1-x}Al_xAs$ layers. In this respect, a clarification of thin superlattice spacer influence,[39] in inverted heterojunctions, is needed since Si as C are likely to be trapped by a superlattice spacer.

ACKNOWLEDGMENT

We would like to thank Dr. G. Bastard for numerous valuable discussions.

[1]T. Ando, A. B. Fowler, and F. Stern, Rev. Mod. Phys. **54**, 438 (1982).
[2]S. Hiyamizu, J. Saito, K. Nanbu, and T. Ishikawa, Jpn. J. Appl. Phys. **22**, L609 (1983).
[3]K. Inoue and H. Sakaki, Jpn. J. Appl. Phys. **23**, L61 (1984).
[4]R. Dingle, H. L. Stormer, A. C. Gossard, and W. Wiegmann, Appl. Phys. Lett. **33**, 665 (1978).
[5]H. L. Stormer, A. Pinczuck, A. C. Gossard, and W. Wiegmann, Appl. Phys. Lett. **38**, 691 (1981).
[6]K. Inoue, H. Sakaki, and J. Yoshino, Jpn. J. Appl. Phys. **23**, L767 (1984).
[7]K. Inoue, H. Sakaki, and J. Yoshino, Appl. Phys. Lett. **47**, 614 (1985).
[8]S. Sasa, J. Saito, K. Nanbu, T. Ishikawa, S. Hiyamizu, and M. Inoue, Jpn. J. Appl. Phys. **24**, L281 (1985).
[9]R. C. Miller, W. T. Tsang, and O. Munteanu, Appl. Phys. Lett. **41**, 374 (1982); R. C. Miller, A. C. Gossard, W. T. Tsang, and O. Munteanu, Phys. Rev. B **25**, 3871 (1982).
[10]S. Sasa, J. Saito, K. Nanbu, T. Ishikawa, and S. Hiyamizu, Jpn. J. Appl. Phys. **23**, L573 (1984).
[11]W. J. Schaff, P. A. Maki, L. F. Eastman, L. Rathbun, B. C. De Cooman, and C. B. Carter, Mater. Res. Soc. Symp. Proc. **37**, 15 (1985).
[12]F. Stern, Phys. Rev. Lett. **44**, 1469 (1980).
[13]C. Guillemot, Phys. Rev. B **31**, 1428 (1985).
[14]G. Bastard, Phys. Rev. B **24**, 5693 (1981).
[15]P. J. Price, Ann. Phys. (N. Y.) **133**, 217 (1981).
[16]M. A. Brummell, M. A. Hopkins, R. J. Nicholas, J. J. Harris, and C. T. Foxon, in Proceedings of the Eighteenth International Conference on the Physics of Semiconductors, Stockholm, 1986 (unpublished).
[17]T. Ando, J. Phys. Soc. Jpn. **51**, 3900 (1982).
[18]P. F. Maldague, Surf. Sci. **73**, 296 (1978).
[19]E. E. Mendez, P. J. Price, and M. Heiblum, Appl. Phys. Lett. **45**, 294 (1984).
[20]B. J. F. Lin, D. C. Tsui, and G. Weimann, Solid State Commun. **56**, 287 (1985).
[21]M. A. Paalanen, D. C. Tsui, A. C. Gossard, and J. C. M. Hwang, Phys. Rev. B **29**, 6003 (1984).
[22]J. P. Harrang, R. J. Higgins, R. K. Goodall, P. R. Jay, M. Laviron, and P. Delescluse, Phys. Rev. B **32**, 8126 (1985).
[23]F. Stern and W. E. Howard, Phys. Rev. **163**, 816 (1967).
[24]J. Kervarec, M. Baudet, J. Caulet, P. Auvray, J. Y. Emery, and A. Regreny, J. Appl. Crystallogr. **17**, 196 (1984).
[25]R. C. Miller, D. A. Kleinman, and A. C. Gossard, Phys. Rev. B **29**, 7085 (1984).
[26]P. M. Petroff, R. C. Miller, A. C. Gossard, and W. Wiegmann, Appl. Phys. Lett. **44**, 217 (1984).
[27]K. Hirakawa and H. Sakaki, Appl. Phys. Lett. **49**, 889 (1986).
[28]W. Walukiewicz, H. E. Ruda, J. Lagowsky, and H. C. Gatos, Phys. Rev. B **29**, 4818 (1984).
[29]H. L. Lee, D. Vakhshoori, Y. H. Lo, and S. Wang, J. Appl. Phys. **57**, 4814 (1985).
[30]H. L. Lee, J. Basinsky, L. Y. Juravel, and J. C. Wooley, Can. J. Phys. **57**, 233 (1979).
[31]S. A. Barnett and J. E. Greene, Surf. Sci. **151**, 67 (1985).
[32]A. Rockett, J. Klem, S. A. Barnett, J. E. Greene, and H. Morkoç, J. Vac. Sci. Technol. B **4**, 519 (1986).
[33]N. C. Jarosik, B. D. McCombe, B. V. Shanabrook, J. Comas, J. Ralston, and G. Wicks, Phys. Rev. Lett. **54**, 1283 (1985); R. J. Wagner, B. V. Shanabrook, J. E. Furneaux, J. Comas, N. C. Jarosik, and B. D. McCombe, Proceedings of the 10th International Conference on Gallium Arsenide and Related Compounds, Biarritz, 1984 (unpublished), p. 315.
[34]F. Stern, Surf. Sci. **58**, 162 (1976).
[35]N. Sano, H. Kato, and S. Chika, Solid State Commun. **49**, 123 (1984).
[36]T. Tanaka, H. Sakaki, and J. Yoshino, Jpn. J. Appl. Phys. **25**, L155 (1986).
[37]P. J. Price and F. Stern, Surf. Sci. **132**, 577 (1983).
[38]B. Deveaud, A. Regreny, J. Y. Emery, and A. Chomette, J. Appl. Phys. **59**, 1633 (1986).
[39]T. J. Drummond, J. Klem, D. Arnold, R. Fischer, R. E. Thorne, W. G. Lyons, and H. Morkoç, Appl. Phys. Lett. **42**, 615 (1983); W. T. Masselink, M. V. Klein, Y. L. Sun, Y. C. Chang, R. Fisher, T. J. Drummond, and H. Markoç, *ibid.* **44**, 435 (1984).